# Self organising map based region of interest labelling for automated defect identification in large sewer pipe image collections

Hiran Ganegedara
Clayton School of IT
Monash University
Australia
Email: hiran.ganegedara@monash.edu

Damminda Alahakoon
Clayton School of IT
Monash University
Australia
Email: damminda.alahakoon@monash.edu

John Mashford
Commonwealth Scientific and
Industrial Research Organisation
Australia
Email: John.Mashford@csiro.au

Andrew Paplinski
Clayton School of IT
Monash University
Australia
Email: andrew.paplinski@monash.edu

Karsten Müller
Research Institute for Water
and Waste Management
RWTH Aachen University
Germany
Email: mueller@fiw.rwth-aachen.de

Thomas M. Deserno
Department of Medical Informatics
RWTH Aachen University
Germany
Email: deserno@ieee.org

***Abstract*—Proper maintenance of sewer pipes is vital for the healthy functioning of a city. Due to the difficulty of reach for sewage pipes, automating pipe inspection has high potential in providing an efficient and objective identification of defects which could lead to damaging the pipe system. A popular approach has been to send remote controlled robots to photograph the pipes and process the images to identify possible defects. However majority of the images contain regular pipe features such as the flow line, pipe joints and pipe connections. Regular features pose a challenge for automated defect detection algorithms which require high processing time. This paper proposes a self organising map based approach to leverage the regularity of image features to isolate regions of interest which could contain defects. As a result, the search space is narrowed down for the defect detection algorithms, decreasing the overall processing time. Novelty of the work lies in the feature extraction and the gradual isolation of the potential defective image features to a manageable size. Therefore, this technique is suitable for large scale real applications. We demonstrate the effectiveness of the proposed approach for a real pipe image data set.**

***Index Terms*—Sewer pipe defect identification, growing self-organising maps, hierarchical clustering**

## I. Introduction

Disposal of waste is an integral component of modern civilisation. Sewer pipe systems enable the flow of waste matter to the relevant processing or disposal centres. Therefore, healthy functioning of sewer pipe systems is essential for the sanitation of cities. Inspecting sewer pipes for defects pose an important task in proper maintenance of sewer pipe systems. Timely identification of defects is critical for fixing the system before any serious damage occurs.

Since most of the sewer pipes are laid underground, pipe inspection is mostly done using remote controlled robots. Imaging devices on the robots capture pipe images as the robot travels along the pipe. Several robot platforms have been proposed for automated sewer pipe inspection[1], [2]. Images acquired by the robots are transferred for evaluation either in real-time or periodically.

Different types of features could be identified in sewer pipes. The most prominent features are the flow lines, pipe joints and pipe connections. In addition, different types of defects could be identified, the main types being corrosions and pipe cracks. Fig. 1 shows an example of an image acquired by an inspection device. Pipe images tend to contain a wide variety of conditions and defects due to a number of parameters. Pipe construction material and pipe surrounding environment are two key factors determining the average colour, contrast and defect types.

Traditionally, defect identification was performed by human inspectors. However, use of human operators has several disadvantages such as high cost, subjectivity and human errors. Therefore much research has been done on automating the defect identification process in sewer pipe inspection.

Fully automating defect identification in sewer pipe images tends to be extremely challenging due to varying pipe conditions and features. A number of techniques have been proposed for defect identification in pipe images[3], [4], [2], [5], [6]. Although none of these techniques are fully automated, [3] proposes an effective method for defect identification using morphological operators and support vector machines (SVMs) [7].

However, in order to improve the accuracy of defect detection, most of the current techniques rely on computationally expensive operations. For example, [3] provides an effective technique for defect detection. However, the time required is high due to the use of SVMs. As a result, processing large

978-1-4673-1490-9/12/$31.00 ©2012 IEEE

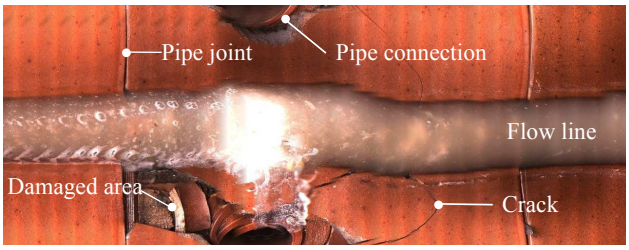


Fig. 1. Features identified in pipe images

image collections tend to take significant amounts of time and could be impractical.

By observing the features of sewer pipe image collections, it is evident that most of the image has regular repetitive features such as pipe segments with flow line, pipe joints and pipe connections. In real data sets, the number of regions of interest which could contain defects is a very low proportion of total image content. Ideally, the defect detection should only be performed on these regions of interest.

This paper proposes a semi-supervised approach to isolate regions of interest in pipe images. Features are generated for the images enabling the identification of repetitive features. A hierarchical self-organising map [8] structure is used to filter the regular, repetitive image features to identify regions of interest. This significantly reduces the amount of image content that needs to be processed for defect identification. Once the search space is narrowed down, time consuming processing techniques can then be used on regions of interest. As a result, the overall time consumption of the process is significantly decreased.

This paper is organised as follows: Section II describes the background theories behind the proposed algorithm followed by Section III, providing a comprehensive description of the proposed algorithm. Section IV evaluates the proposed technique with experiments and results presented. Section V discusses the implications and future work.

## II. Background

The proposed technique has two phases, feature extraction and clustering. Feature extraction is based on the Canny edge detection [9] algorithm and clustering is performed by self-organising maps. This section describes the Canny edge detection algorithm and self-organising maps.

### A. Canny edge detection algorithm

The Canny edge detector is a widely used technique for edge identification in images. The motivation behind the Canny edge detector was to identify the optimum edges by:

1) detection - the algorithm should identify as many true edges as possible
2) localisation - the detected edges should be as close as possible to the edges in the image
3) response - an edge should be identified only once and image noise should not result in false positives

The algorithm operates in multiple stages and uses non-maximum suppression to localise edges. Following is a brief description about the stages in Canny edge detection algorithm.

*1) Smoothing:* Image is smoothened in order to remove any random noise. The most common smoothing technique used is Gaussian smoothing.

*2) Intensity gradient calculation:* Gradient intensities of the smoothed image are calculated in horizontal and vertical directions. Different techniques could be used to calculate intensity gradients such as Sobel operator, Roberts' cross and Prewitt operator. Using the horizontal and vertical components, magnitude and orientation of edges are calculated. Orientation values are rounded to the nearest 0°, 45°, 90°, 135° angles.

*3) Non-maximum suppression:* A pixel value is retained if its two neighbouring pixels along the same orientation have lesser values, otherwise the value is set to 0. This step suppresses any residual edges detected along a main edge.

*4) Thresholding:* The final edge detected image is obtained by thresholding the image with two thresholds, lower and upper. If the magnitude of the edge strength is less than the lower threshold, its value is set to 0. Similarly, if the magnitude of the edge strength is greater than the upper threshold, the value is set to 1. Depending on the application requirement, the range between lower and upper threshold values could be set to a value in the range of (0,1). Determining the threshold values is application specific.

### B. Self organising maps

The Self-Organising Map (SOM) [8] is an unsupervised learning algorithm. While the primary feature of the SOM is to visualise high dimensional data in low dimensional space, SOMs are also used for clustering and pattern recognition. The SOM starts with a lattice (mostly rectangular or hexagonal) of neurons for which input vectors are presented randomly. For each input vector, the best matching unit (BMU) is identified and the BMU's weight is adjusted towards the input vector following the Hebbian learning rule. The input data set is presented over a number of iterations at the end of which the map of neurons are topologically arranged to form a summarised view of the data set in low dimensional space.

While the SOM provides an effective framework for visualising high dimensional data sets, deciding the size of the lattice could pose a challenge especially for large data sets. Since the running time of the SOM algorithm significantly increases with the number of input vectors, finding the optimum lattice size by trial and error could be impractical. A later extension to SOM called the Growing Self-Organising Map (GSOM) [10] overcomes this issue by having to specify only one parameter, the *spread factor*. The GSOM algorithm has two phases, the growing phase and the smoothing phase. The GSOM algorithm operates by starting with only four neurons and by growing neurons to match the data set. Neurons are grown if the accumulated quantisation error is greater than a defined threshold called the *growth threshold (GT)*. $GT$ is determined

by the number of dimensions, $d$ and the spread factor, $SF$ given by Equation (1).

$$GT = -d \times \ln(SF) \tag{1}$$

The smoothing phase is similar to that of SOM where the weight vectors of the BMU and its neighbours are adapted towards the input vectors over a number of iterations.

Recently, a scalable approach has been proposed for large scale data clustering using the SOM algorithm[11]. The number of vectors for image data sets could be extremely high for large image collections. The Parallel GSOM proposed in [11] provides a framework for utilising parallel computing to process large data sets.

## III. Methodology

A reasonably well maintained sewer pipe system would result in image collections containing a majority of undamaged or "good" pipe segments. As a result, the majority of the image content could be discarded due to absence of defects. However, proper identification such content is critical since labelling a defect as non defective (true negative) could lead to pipe damage. As a result, labelling a non defective image as defective (false positive) is considered far less severe than false negatives.

Fig. 2 shows the overall architecture of the proposed approach. In summary, the proposed algorithm generates features for the image collection and hierarchically clusters the image features to separate regular and irregular features. Features are generated from pixel gradient values by Canny like edge detection mechanism due to its effectiveness and faster operation [12]. GSOMs are used to classify the generated features as regular and irregular. Thus the algorithm consists of three phases, pre-processing, feature extraction and clustering.

### A. Pre-processing

In order to ensure smooth clustering, feature extraction process should have a low signal to noise ratio. Noise could be caused by the texture and markings in the pipe as well as by the imaging sensor on the image acquisition device. Noise is reduced in two steps using scaling down and smoothing.

*1) Image scaling:* Any noise caused by irrelevant pipe features such as deposits, markings and pipe texture is reduced by scaling the image to 10% of its original height. The objective of the scaling step is to ensure that any irrelevant image features are suppressed and relevant features are preserved. Since edge detection is used as the primary feature generation technique, any defects that remain should consist of detectable edges. By visual inspection of the image collection, it was determined that at 10% of the original height, the images still preserve any defects that should be identified.

The image collection used for this paper consisted of a mean height of 500 pixels, thus the images were scaled to a height of 50 pixels. In order to minimise visual distortion and for efficient performance, bilinear interpolation was used as the scaling technique.

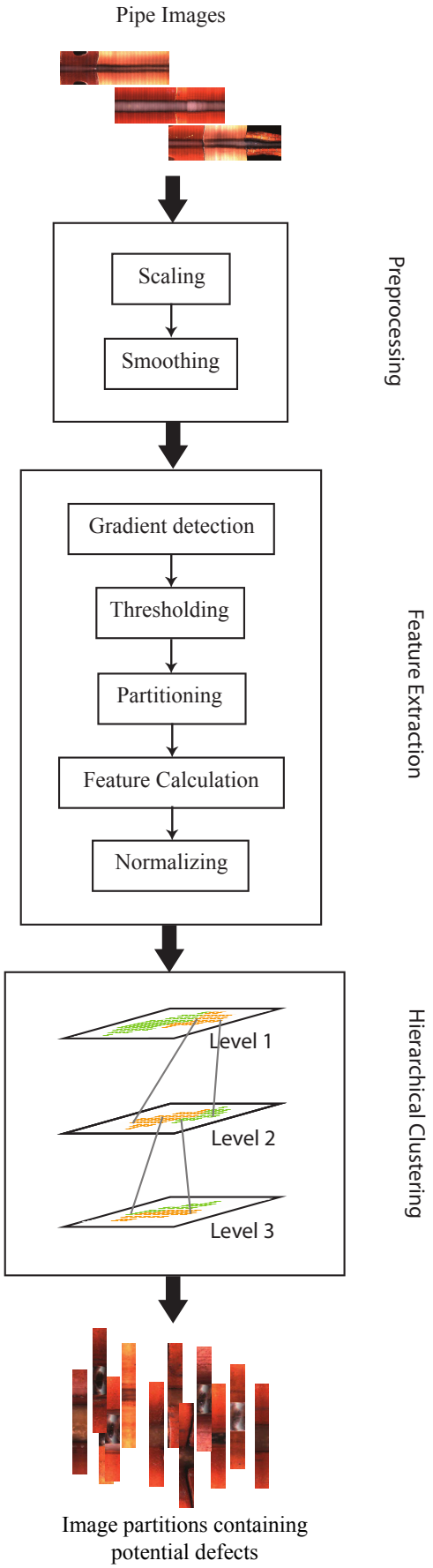


Fig. 2. Overview of the proposed approach

*2) Smoothing:* Due to defects in imaging sensors and post processing techniques, random noise could be added to the images. Since features are extracted by examining the edge strength, such noise could lead to false positives. In order to suppress random noise, image could be smoothened by comparing pixel values to that of it's neighbours. Gaussian smoothing is a widely used technique for image smoothing. Therefore, pipe images are smoothened by convolving with a Gaussian kernel. Since the smoothing operation is performed on the scaled down image, performance tend to be significantly faster compared with smoothing the full size image.

### B. Feature extraction

A Canny edge detector based process is used to calculate the features for each image by partitioning the image into parts with equal length. Each partition is then convolved with Sobel operators in horizontal and vertical directions to calculate the edge strength for each pixel which is followed by double thresholding. The image is divided into blocks and the root mean square (RMS) edge strength and the standard deviation for each block is calculated as the feature vector.

*1) Image partitioning:* Images acquired from pipe inspection devices tend to be of varying lengths ranging from approximately 6,000 pixels to 50,000 pixels. As a result, images are partitioned into even length blocks spanning the entire height for feature extraction, which provides a uniform basis for image feature representation. The block length was determined as five pixels (which scales to 50 pixels in the full size image) which is sufficiently large to contain a single defect. In order to compensate for boundary effects such as pipe features separating at the boundary, a one pixel overlap was introduced. Partitioning of the images was performed at a logical level such that convolution operators could process the partitions beyond the boundary.

Fig. 3 shows a sample of the image partitions generated in the partitioning process.

*2) Edge detection:* Sobel operators are used for edge strength calculation using pixel gradient values. Horizontal operator ($G_x$) and vertical operator ($G_y$) are given by equation (2) for completeness. Each image partition is convolved with Sobel operators in the horizontal and vertical directions.

$$G_x = \begin{bmatrix} -1 & 0 & +1 \\ -2 & 0 & +2 \\ -1 & 0 & +1 \end{bmatrix}, G_y = \begin{bmatrix} -1 & -2 & -1 \\ 0 & 0 & 0 \\ +1 & +2 & +1 \end{bmatrix} \quad (2)$$

The main limitation of applying the Sobel operators to five pixel wide partitions is the effect of distortion due to applying the convolution operator at the borders. In order to prevent the distortion from border effects Sobel operators are applied to the unpartitioned image and edge strengths relevant to each image partition is obtained.

At the end of the edge detection process, two matrices are created for each image partition containing the edge strengths in horizontal and vertical directions.

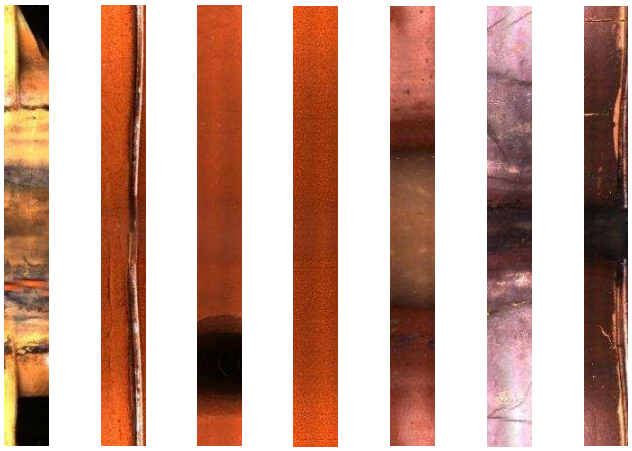


Fig. 3. Example image partitions containing different image features. (A) - A segment with noise (B) - pipe joint, (C) - pipe connection, (D) - pipe segment with a smooth flow line, (E) - clear flow line, (F) - pipe segment with cracks, (G) - pipe joint with defect at the top

*3) Thresholding:* Similar to Canny edge detection, double thresholding is performed on the edge detected image in order to suppress weak edges and to normalise strong edges. The thresholds were selected by trial and error so that relevant image features are retained. Any value less than the lower threshold is set to 0, values between lower and upper threshold are set to 0.5 and values greater than the upper threshold are set to 1. Due to the thresholding process, pixels that could lead to false positives are reduced.

*4) Feature calculation:* After the thresholding process, each image partition is divided into five equal blocks along the vertical axis. For example, if the height of the image is 50 pixels, each block would have a height of 10 pixels. The feature vectors are calculated using the root mean square (RMS) and standard deviation ($\sigma$) statistical measures. The RMS value is an indication of how strong the edges are in a particular orientation. $\sigma$ is an indication of the degree of fluctuation of the edge strengths. For example, a high $\sigma$ value could indicate a pipe connection where a circular pattern is shown on the image. Table. I summarises some of the possible features that could be identified using this feature set. When these feature values are associated with the block location, provides a more powerful basis for defect identification.

TABLE I
POSSIBLE PIPE FEATURES RECOGNISED BY FEATURE VECTOR VALUES

| Feature type | Horizontal | | Vertical | |
|---|---|---|---|---|
| | RMS | $\sigma$ | RMS | $\sigma$ |
| Flow line | High | Medium | Low | Low |
| Flow line with defect | High | High | Low | Medium |
| Pipe joint | Low | Low | High | Medium |
| Defective pipe joint | Low | Medium | High | High |
| Pipe connection | Medium | High | Medium | High |
| Defective connection | High | High | High | High |

Once the calculations are completed, each image block is represented using four features. RMS and $\sigma$ of edge strengths in both horizontal and vertical directions. Since five blocks are created for each image partition, each image partition is represented as a vector with 20 feature values.

At the end of the feature calculation process, vectors are created for each image partition. The feature vectors are normalised since SOM based techniques require input vectors with values in [0,1].

### C. Hierarchical clustering

The objective of the hierarchical clustering phase is to filter out the regular image features in each level so that irregular features could be identified. The GSOM is used as the learning technique due to its suitability for exploratory data analysis.

Due to multiple characteristics such as flow lines, pipe connections, variations in lighting, pipe joints, defects etc, a gradual filtering approach was found to be more effective rather than a single pass clustering. A cluster hierarchy was chosen as opposed to identifying multiple clusters on a single level due to the following reasons.

1) The number of input vectors containing defects is extremely low. As a result, the defect cluster would be under represented.
2) The cluster distribution is uneven with approximately 50% of the image partitions containing only flow lines, approximately 25% containing pipe joints, approximately 10% containing pipe connections and the remainder containing defects and other features. Cluster accuracy of SOMs tends to decrease in the presence of uneven cluster distributions.
3) It is easier to backtrack and search in the previous level for defects if required as opposed to searching the entire input space.

Therefore, a three level hierarchy was created having two clusters at each level. The two clusters could be loosely named regular and irregular pipe image partitions. The input vectors mapped to the irregular cluster are used as input to create the next level GSOM which is again separated into two clusters. Similar to the first level, the clusters are labelled as regular and irregular and the input vectors mapped to the irregular cluster is used as input to the third and final level. The third level GSOM is also clustered into regular and irregular image partitions and the irregular cluster is considered as likely to contain image partitions that contain defects.

*1) Cluster separation:* Neurons in the GSOM at each level of the hierarchy were clustered using the k-means algorithm[13]. K-means algorithm was used to form two clusters from the neurons in the GSOM. The DB-Index was calculated for each cluster to find the optimum clustering[14]. The cluster configuration with the lowest DB-Index value was considered as the optimum for the map. The two clusters were then visually inspected and labelled as regular and irregular.

## IV. Experiments and results

The effectiveness of the proposed technique was evaluated using a real pipe image data set.

### A. Data set

The image data set consisted of 66 unwrapped images of real sewer pipes using the Panoramo© system. The image lengths vary from 3840 pixels to 50400 pixels which resulted in different number of partitions for each image. The image data set was divided into 30 training images and 36 test images. The training set was selected at random such that a reasonable mix of image features was distributed across both sets.

Features were extracted for both sets using the proposed approach. The training set consisted of 18649 feature vectors whereas the test set contained 28059 feature vectors. Each vector consisted of 20 feature values. The test set was manually inspected and the defects were labelled.

### B. Results

The cluster hierarchy was generated using the features extracted from the training image set and the clusters were manually annotated as regular and irregular. The test image feature set was then fed as input to the cluster hierarchy and the vectors that were mapped to the irregular cluster at the top level were examined. It was observed that 100% of the defects labelled in the training set were contained in the irregular cluster. The results of the test image classification are shown in Fig. 4.

It could be observed that the level 1 GSOM acts as a filter for image partitions with clear flow lines. When the map was separated into two clusters, reasonable regular and irregular feature separation could be observed. Since the goal was to minimise false negatives, the irregular feature cluster contained more vectors. The cluster distribution was 11100 (40%) vectors in the regular feature cluster and 16959 (60%) vectors in the irregular feature cluster. The primary feature in the regular feature cluster was high RMS and low $\sigma$ values for horizontal edges and low RMS and low $\sigma$ values for vertical edges. In terms of image features, the regular feature cluster contained clearly detectable flow lines which contribute to approximately 50% of the total image features. In addition, the regular feature cluster also contained blank image partitions which could be found at the left and right boundaries of the images. The irregular cluster consisted of varying flow lines, pipe connections, pipe joints and partitions with distorted content. In summary, the level 1 of the cluster hierarchy separated clear flow lines and input vectors that do not get classified as flow lines were presented as input to the next level.

The reason for some flow line features being classified as irregular in level 1 is due to the nature of feature value distribution. For example, a wider flow line could span several image blocks whereas a narrow flow line could span only the centre block. If the number of vectors representing narrow flow lines is considerably higher compared to features representing

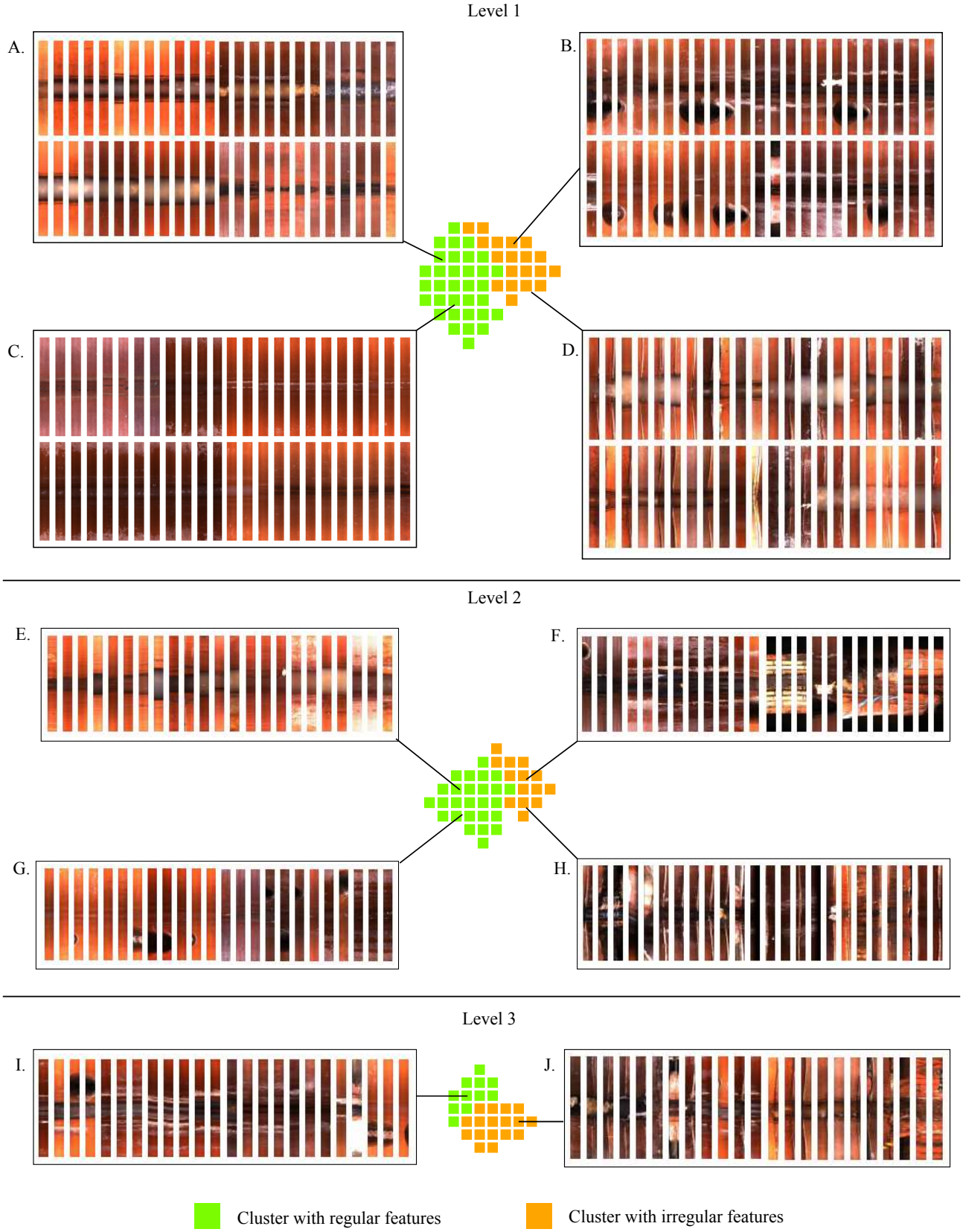


Fig. 4. Image distribution at different levels of the hierarchy. (A) - a neuron containing thick flow line features (B) - a neuron containing pipe connection features, (C) - a neuron containing thin flow line features, (D) - a neuron containing pipe joint features, (E) - A neuron containing flow line features, (F) - a neuron containing distorted pipe connection features, (G) - a neuron containing proper pipe connection features, (H) - a neuron containing pipe joint features, (I) - a neuron containing regular features, (J) a neuron containing irregular features

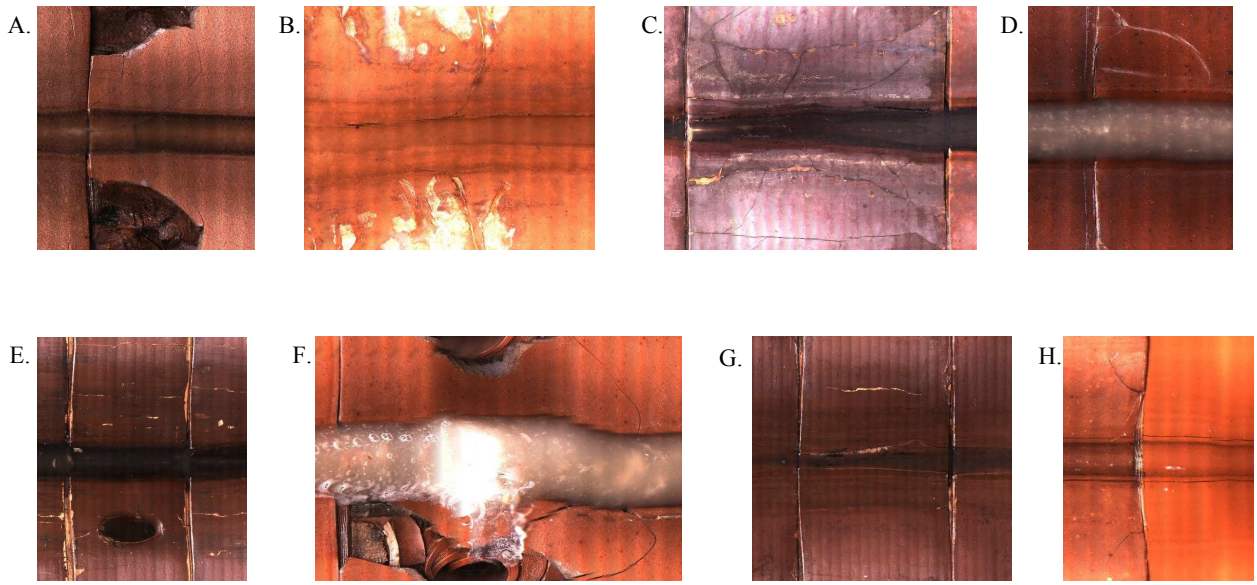


Fig. 5. Defects captured in the level 3 irregular feature cluster. (A, D, H) - Defects at pipe joints (B) - vertical cracks, (C) - cracked pipe segment, (E) - horizontal crack, (F) - Defects at pipe connection, (F)

wider flow lines, wider flow lines tend to be marked as irregular. However, after most of the narrow flow lines are filtered out from the data set which is input to next level, wider flow lines tend to get classified as regular due to the relatively higher presence. This effect was observed in level 2.

Level 2 of the cluster hierarchy acted as a filter for further flow lines and other regular features such as pipe connections without distortions. The regular feature cluster contained 10261 (61%) of the vectors. The irregular feature cluster contained image partitions with higher distortions and contained 6698 (39%) of the vectors. The vectors mapped to the irregular feature cluster were input to the GSOM trained at level 3.

The final level of the cluster hierarchy further filtered the input space. It could be observed that the image partitions mapped to the regular feature cluster contained jagged flow lines and markings. The irregular feature cluster also contained more distorted image partitions than the previous level. The regular feature cluster contained 2973 (44%) of the vectors whereas the irregular feature cluster contained the remaining 3725 (56%).

Inspecting the image partitions mapped to regular and irregular feature clusters in the three levels, it could be seen that the level or distortion in the images increases as the number of levels increases. Thus it demonstrates the algorithm's effectiveness in progressively filtering out regular image features to isolate image partitions that could contain defects.

Accuracy of clustering was evaluated using manually labelled defects in the test set. It was observed that all the defects were present in the irregular cluster at level 3. Fig. 5 shows some of the identified defects.

In summary, the proposed approach narrowed down the search space from an initial 28059 vectors to 3725 vectors which is a reduction of 86.7%. This significant reduction of the search space could lead to faster detection of defects. Efficiency of the algorithm is high since the features are extracted from scaled down images. In addition, the time requirement for classifying vectors on an already trained neural network is very low. The training of the networks could be improved by using the scalable approach suggested in [11]

## V. Discussion

It is evident that the proposed technique has significantly narrowed down the search space for defect detection. In addition all the identified defects in the test data set were included in the irregular feature cluster at level 3 indicating high accuracy of the proposed approach. As a result, defect identification algorithms which possess high time complexities could benefit from having to process a small subset of the total image collection.

The proposed technique could be further improved by incorporating current flow line detection techniques (e.g.: [15] to filter out flow line image partitions. Since image partitions containing flow lines form majority of the image partitions, flow line detection could yield to faster performance and more accurate results. In addition, the number of levels in the cluster hierarchy could also be reduced.

For processing very large image collections, the proposed approach could be scaled to be executed on distributed computing platforms. Pre-processing and feature generation could easily be parallelised since each image is considered independent from others. A scalable approach could be utilised for training of GSOMs and generation of the cluster hierarchy using work proposed in [11].

## REFERENCES


[1] H. Kuntze, H. Haffner, M. Selig, D. Schmidt, K. Janotta, and M. Loh, "Development of a flexible utilisable robot for intelligent sensor-based sewer inspection," 1994, pp. 367–374.

[2] R. Kirkham, P. Kearney, K. Rogers, and J. Mashford, "PIRAT - a system for quantitative sewer pipe assessment," *The International Journal of Robotics Research*, vol. 19, no. 11, p. 1033, 2000.

[3] J. Mashford, M. Rahilly, P. Davis, and S. Burn, "A morphological approach to pipe image interpretation based on segmentation by support vector machine," *Automation in Construction*, vol. 19, no. 7, pp. 875–883, 2010.

[4] O. Duran, K. Althoefer, and L. Seneviratne, "Automated pipe defect detection and categorization using camera/laser-based profiler and artificial neural network," *Automation Science and Engineering, IEEE Transactions on*, vol. 4, no. 1, pp. 118–126, 2007.

[5] S. Sinha and F. Karray, "Classification of underground pipe scanned images using feature extraction and neuro-fuzzy algorithm," *Neural Networks, IEEE Transactions on*, vol. 13, no. 2, pp. 393–401, 2002.

[6] O. Moselhi and T. Shehab-Eldeen, "Classification of defects in sewer pipes using neural networks," *Journal of infrastructure systems*, vol. 6, p. 97, 2000.

[7] C. Cortes and V. Vapnik, "Support-vector networks," *Machine learning*, vol. 20, no. 3, pp. 273–297, 1995.

[8] T. Kohonen, "The self-organizing map," *Proceedings of the IEEE*, vol. 78, no. 9, pp. 1464–1480, 1990.

[9] J. Canny, "A computational approach to edge detection," *Pattern Analysis and Machine Intelligence, IEEE Transactions on*, no. 6, pp. 679–698, 1986.

[10] D. Alahakoon, S. Halgamuge, and B. Srinivasan, "Dynamic self-organizing maps with controlled growth for knowledge discovery," *Neural Networks, IEEE Transactions on*, vol. 11, no. 3, pp. 601–614, 2000.

[11] H. Ganegedara and D. Alahakoon, "Scalable data clustering: A Sammon's projection based technique for merging GSOMs." Springer, 2011, pp. 193–202.

[12] M. Sharifi, M. Fathy, and M. Mahmoudi, "A classified and comparative study of edge detection algorithms." IEEE, 2002, pp. 117–120.

[13] J. MacQueen, "Some methods for classification and analysis of multivariate observations," vol. 1. California, USA, 1967, p. 14.

[14] N. Ahmad, D. Alahakoon, and R. Chau, "Cluster identification and separation in the growing self-organizing map: application in protein sequence classification," *Neural Computing & Applications*, vol. 19, no. 4, pp. 531–542, 2010.

[15] S. Kirstein, K. Muller, M. Walecki-Mingers, and T. Deserno, "Robust adaptive flow line detection in sewer pipes," *Automation in Construction*, vol. 21, pp. 24–31, 2011.